Iranian Journal of Numerical Analysis and Optimization
Vol. 14, No. 4, 2024, pp 1247–1279
https://doi.org/10.22067/ijnao.2024.88781.1472
https://ijnao.um.ac.ir/

Research Article

A novel mid-point upwind scheme for fractional-order singularly perturbed convection-diffusion delay differential equation

N.A. Endrie*, and G.F. Duressa

Abstract

This study presents a numerical approach for solving temporal fractional-order singularly perturbed parabolic convection-diffusion differential equations with a delay using a uniformly convergent scheme. We use the asymptotic analysis of the problem to offer a priori bounds on the exact solution and its derivatives. To discretize the problem, we use the implicit Euler technique on a uniform mesh in time and the midpoint upwind finite difference approach on a piece-wise uniform mesh in space. The proposed

*Corresponding author

Received 2 July 2024; revised 5 August 2024; accepted 19 August 2024

Nuru Ahmed Endrie
Department of Mathematics, College of Natural and Computational Science, Arba Minch University, Arba Minch, Ethiopia. e-mail: nuruahmed222@gmail.com

Gemechis File Duressa
Department of Mathematics,College of Natural and Computational Science, Arba Minch University, Arba Minch, Ethiopia and
Department of Mathematics, College of Natural and Computational Science, Jimma University, Jimma, Ethiopia. e-mail: gammeef@gmail.com

How to cite this article
Endrie, N.A. and Duressa, G.F., A novel mid-point upwind scheme for fractional-order singularly perturbed convection-diffusion delay differential equation. *Iran. J. Numer. Anal. Optim.*, 2024; 14(4): 1247-1279. https://doi.org/10.22067/ijnao.2024.88781.1472

technique has a nearly first-order uniform convergence order in both spatial and temporal dimensions. To validate the theoretical analysis of the scheme, two numerical test situations for various values of ε are explored.

AMS subject classifications (2020): Primary 65L11; Secondary 65N12.

Keywords: Caputo–Fabrizio derivative operator, midpoint upwind scheme, fractional-order differential equation, delay differential equation, singularly perturbed problem.

1 Introduction

This work examines the singularly perturbed delay parabolic differential equation involving fractional order in time

$$\begin{aligned} \mathcal{L}w(s,t) \equiv^{Cf} D_t^{\gamma} w(s,t) - \varepsilon \frac{\partial^2 w(s,t)}{\partial s^2} + a(s)\frac{\partial w(s,t)}{\partial s} + b(s,t)w(s,t) \\ = -c(s,t)w(s,t-\delta) + f(s,t), \qquad (s,t) \in \Omega = (0,1)\times(0,\mathfrak{T}] \end{aligned} \tag{1}$$

with

$$\begin{cases} w(s,t) = \varphi_b(s,t), & \text{for}(s,t) \in [0,1]\times[-\delta,0], \\ w(0,t) = \varphi_l(t), w(1,t) = \varphi_r(t), & \text{for } \ t \in (0,\mathfrak{T}), \end{cases} \tag{2}$$

where $\varepsilon (0 < \varepsilon \ll 1)$ is a singular perturbation parameter, δ is a delay parameter, and the Caputo–Fabrizio fractional derivative of order $0 < \gamma < 1$ is denoted by ${}^{CF}D_t^{\gamma}$. The solution of the problem (1) possesses a boundary layer of regular type at $s = 1$ of width $\mathcal{O}(\varepsilon)$ if $a(s) \geq \beta > 0, b(s,t) \geq 0$, $c(s,t) \geq \alpha > 0$ and they are smooth and bounded on the domain $\bar{\Omega} = [0,1]\times[0,\mathfrak{T}]$, and to avoid oscillations in the solution, we take $b(s,t) + c(s,t) \geq \theta$.

In contrast to its classical equivalents, a number of scientists and academics are showing the effectiveness of fractional derivative and integral operators in analyzing and modeling real-world occurrences. Throughout recent years, fractional calculus has been studied because it illustrates memory quality. Time-fractional advection-diffusion equations, time-fractional Burgers equations, and other models have been developed by applying fractional partial differential equations to model problems in a wide range of fields,

such as control theory, chemical physics, engineering, medicine, stochastic processes, and biology [20, 38, 32].

Caputo fractional derivatives are employed to explain most mathematical models for such systems. The main argument in favor of the Caputo fractional derivative is that the beginning conditions have the same form as the differential equations of integer order at time $t = 0$. On the other hand, the Riemann–Liouville technique necessitates initial conditions that include the limit values of the Riemann–Liouville fractional derivative at the initial time $t = 0$. These criteria are not entirely apparent in terms of their physical interpretation. On the contrary, the Riemann–Liouville fractional derivative may give the Caputo fractional derivative with certain assumptions about the regularity of the function [27]. To overcome the singularity of the kernel, Caputo and Fabricio devised a new fractional derivative in response to these difficulties and inconveniences. One of the intriguing characteristics of this novel fractional derivative is the presence of an exponential kernel, which can construct and characterize structures at various scales. Further benefits are gained in certainly published journals using this new fractional derivative operator for the analysis of the groundwater contamination problem, the nonlinear Fisher's reaction-diffusion problem, and the magneto hydrodynamics free convection flow [4, 19, 29].

Singularly perturbed delay differential equations (SPDDEs) are employed to model physical problems that evolve based on both their current condition and history. To make a model more realistic, it may be important to represent former system states in addition to the current state. Delay differential equations (DDEs) are useful for describing time-dependent phenomena that rely on a past state [11].

SPDDEs are used to model physical problems whose growth is controlled not only by the system's present state but also by its history. It is occasionally required to comprise past states of the system rather than only the current state in order to make the model more accurate. When the rate of change of a time-dependent phenomenon is dependent on a preceding state, DDEs play an important role in mathematical modeling [10]. The study of DDEs has grown in popularity over the last several decades due to their numerous applications in domains such as bio-sciences, control theory, economics, ma-

terial science, medicine, robotics, and others; see Cooke [5], Diekmann et al. [6], Driver [7], Norkin [26], Kolmanovskii, and Myshkis [15], Hale and Lunel [13], Kolmanovskii and Nosov [16], Kuang [17]. There are various real-world examples of DDEs in the works by Nelson and Perelson [25], Villasana and Radunskaya [37], and Zhao [39].

Because the boundary layer exists in the singularly perturbed problem solution, standard finite difference approaches produce unsuitable numerical results. Various numerical algorithms have been devised to solve these problems, which require a technique known as a uniformly convergent method independent of the perturbation parameter's value. Fitted mesh and fitted operator are the two most used numerical methods to construct a uniformly convergent scheme. Fitted mesh approaches use a layer-adapted nonuniform mesh that is dense in the layer(s), whereas the fitted operator employs an exponentially fitted scheme [31, 14]. However, this highlights the numerical method's computational inefficiency. When the number of mesh points grows, the resulting algebraic system of equations may become ill-conditioned. The shortcoming encourages the creation of a suitable numerical approach whose accuracy is independent of the perturbation parameter, highlighting the key advantage of the proposed method [12].

The number of papers addressing numerical solutions to time-fractional singularly perturbed ordinary differential equations (ODEs) and partial differential equations (PDEs) is rather modest. Bijura [3] offered higher-order asymptotic solutions for fractionally-order nonlinear singular perturbation problems. Roop [30] solved fractional ODEs numerically using the finite element method. Al-Mdallal and Syam [1] applied the Pade approximation to solve nonlinear singularly perturbed two-point boundary-value problems of fractional order. Atangana and Goufo [2] extended the matched asymptotic technique to address fractional-order boundary layer problems. Sayevand and Pichaghchi [35] proposed a method to solve singularly perturbed ODEs in their fractional-order boundary value problem. They defined the local fractional derivative and expanded the matching asymptotic expansion technique using its properties. Sayevand and Pichaghchi [34] developed a linear B-spline operational matrix with fractional derivatives for singularly perturbed ODEs and PDEs. Sahoo and Gupta [33] proposed a finite difference

approach to tackle time-fractional, singularly perturbed convection-diffusion problems. Kumar and Vigo-Aguiar [18] studied delay parabolic and time-fractional SPDEs and created discretized time domains with uniform step size and piece-wise-uniform Shishkin meshes in space domains.

To the best of our knowledge, the development and analysis of a numerical scheme for the class of singularly perturbed fractional-order delay differential equations under discussion is covered in only one publication in the literature [18]. This paper aims to present and analyze a new class of midpoint upwind finite difference methods using piece-wise uniform Shishkin mesh. By preserving significant aspects of the corresponding continuous problems, these techniques produce reliable numerical results.

The succeeding sections of the paper are organized as follows: Section 2 defines the preliminary concepts. Section 3 examines the continuous problem description, including its analytic solution and derivative behavior within stated constraints. Section 4 presents a midpoint upwind numerical scheme based on the Shishkin mesh developed. The method's uniform convergence analysis is discussed in Section 5. Section 6 details the numerical experimentation conducted to validate theoretical results and demonstrate the accuracy of the method. The final section provides a summary of the main conclusions drawn in the paper.

2 Preliminaries

We now offer the definitions and approaches that are required for this study.

Definition 1 (Singularly-perturbed problem)**.** [21] When the highest-order derivative of a differential equation is multiplied by a small parameter ε (where ε is the perturbation parameter, such that $0 < \varepsilon << 1$), the equation is considered singularly perturbed.

Definition 2 (Gamma function)**.** [28] For a complex number z with real part nonnegative ($\mathbb{R}(z) > 0$), the gamma function is defined as

$$\Gamma(z) = \int_0^\infty x^{z-1} e^{-x} dx. \tag{3}$$

Definition 3 (Caputo fractional derivative operator)**.** [28] For $n \in \mathbb{N}$ and $\gamma \in (n-1, n)$, the Caputo fractional derivative of a function $g(t)$ with lower limit zero can be defined as

$$D_0^{\gamma} g(t) = \frac{1}{\Gamma(n-\gamma)} \int_0^t \frac{g^{(n)}(\xi)}{(t-\xi)^{\gamma-n+1}} d\xi. \tag{4}$$

Definition 4 (Caputo–Fabrizio Operator)**.** [4] Considering fractional derivatives with order $\gamma > 0$, a novel operator known as the Caputo–Fabrizio operator is defined as follows:

$${}^{CF}D_{0,t}^{\gamma}(g(t)) = \frac{L(\gamma)}{1-\gamma} \int_0^t g'(\xi) \exp\left[-\gamma \frac{t-\xi}{1-\gamma}\right] d\xi, \tag{5}$$

where $g \in H^1(a,b), b > a$, and $L(\gamma)$ is the normalization functions (any smooth positive function) such that $L(0) = L(1) = 1$. Moreover, we observe that the aforementioned definition does not contain a singular kernel.

3 Properties of continuous problem

Assuming sufficiently smoothness of $\varphi_l(t), \varphi_r(t),$ and $\varphi_b(x,t)$ and satisfying the following compatibility conditions at the corner points $(0,0), (1,0)$ and $(0,-\delta)$ as well as $(1,-\delta)$, the existence and uniqueness of the solution of (1)–(2) can be established.

$$\begin{cases} \varphi_b(0,0) = \varphi_l(0), \\ \varphi_b(1,0) = \varphi_r(0), \end{cases} \tag{6}$$

and

$$\begin{cases} \left.\dfrac{d^{\gamma}\varphi_l}{d^{\gamma}t}\right|_{t=0} - \varepsilon \left.\dfrac{\partial^2 \varphi_b}{\partial x^2}\right|_{(0,0)} + a(0) \left.\dfrac{\partial \varphi_b}{\partial x}\right|_{(0,0)} + b(0,0)\varphi_b(0,0) \\ \quad = -c(0,0)\varphi_b(0,-\delta) + f(0,0), \\ \left.\dfrac{d^{\gamma}\varphi_l}{d^{\gamma}t}\right|_{t=0} - \varepsilon \left.\dfrac{\partial^2 \varphi_b}{\partial x^2}\right|_{(1,0)} + a(1) \left.\dfrac{\partial \varphi_b}{\partial x}\right|_{(1,0)} + b(1,0)\varphi_b(1,0) \\ \quad = -c(1,0)\varphi_b(1,-\delta) + f(1,0). \end{cases} \tag{7}$$

Now, we will show that the operator $\mathfrak{L}$ satisfies the maximum principle.

Lemma 1 (Continuous maximum principle)**.** Consider the function $\phi(s,t) \in C^2(\Omega) \cap C^0(\bar{\Omega})$, with $\mathfrak{L}\phi(s,t) \geq 0$ in Ω and $\phi(s,t) \geq 0$, for all $(s,t) \in \Lambda = \{0\} \times (0,\mathfrak{T}] \cup \{1\} \times (0,\mathfrak{T}] \cup [0,1] \times [-\delta, 0]$. Then $\phi(s,t) \geq 0$, for all $(s,t) \in \bar{\Omega}$.

Proof. Let us assume that there exists $(\varsigma, \iota) \in \bar{\Omega}$ with

$$\phi(\varsigma,\iota) = \min_{(s,t)\in\bar{\Omega}} \phi(s,t), \quad \text{and} \quad \phi(\varsigma,\iota) < 0$$

With respect to these assumptions, we can deduce that $(\varsigma,\iota) \notin \Lambda$, implying that $(\varsigma,\iota) \in \Omega$. Using the operator $\mathfrak{L}$ on $\phi(s,t)$, we get

$$\mathfrak{L}\phi(s,t) = D_t^{\gamma}\phi(x,t) - \varepsilon\phi_{ss}(s,t) + a(s)\phi_s(s,t) + b(s,t)\phi(s,t),$$

At the point of minimum (ς,ι), we obtain

$$\mathfrak{L}\phi((\varsigma,\iota)) = D_t^{\gamma}\phi(\varsigma,\iota) - \varepsilon\phi_{ss}(\varsigma,\iota) + a(\varsigma)\phi_s(\varsigma,\iota) + b(\varsigma,\iota)\phi(\varsigma,\iota).$$

The function ϕ has minima at the point (ς,ι), so $D_t^{\gamma}\phi \geq 0$, $\phi_s = 0$, $\phi_{ss} \geq 0$ at point (ς,ι), and $b(\varsigma,\iota) \geq 0$ for $(\varsigma,\iota) \in \Omega$. Therefore, we have

$$\mathfrak{L}\phi(\varsigma,\iota) < 0.$$

This contradicts our assumption $\mathfrak{L}\phi(s,t)$ in Ω.

Consequently, we conclude that $\phi(s,t) \geq 0$, for all $(s,t) \in \bar{\Omega}$. □

Lemma 2. The differential equation (1)–(2) has a solution $y(s,t)$ that satisfies this estimate:

$$|w(x,t) - \varphi_b(s,0)| \leq Ct, \qquad (x,t) \in \bar{\Omega},$$

in which C is a constant that does not depend on ε.

Proof. See reference [23]. □

Lemma 3. With its initial and boundary conditions in (2), the solution to problem (1) is bounded as

$$|w(s,t)| \leq C, \quad \text{for all } (s,t) \in \bar{\Omega}. \tag{8}$$

Proof. From Lemma 2, we have

$$\begin{aligned}|w(s,t)| &= |w(s,t) - \varphi_b(s,0) + \varphi_b(s,0)| \\ &\leq |w(s,t) - \varphi_b(s,0)| + |\varphi_b(s,0)| \\ &\leq Ct + |\varphi_b(s,0)| \\ &\leq Ct + C \\ &\leq C \qquad \text{since } t \in (0,\mathfrak{T}],\ \text{t is bounded.}\end{aligned}$$

□

Lemma 4. [9] For any nonnegative integers n, m with $0 \leq n+m \leq 5$ and appropriate compatible conditions at the edges, both the regular $v(x,t)$ and singular component $w(x,t)$ satisfy the subsequent bounds:

$$\left|\frac{\partial^{n+m} v(s,t)}{\partial s^n \partial t^m}\right| \leq C\left(1+\varepsilon^{4-n}\right), \tag{9}$$

$$\left|\frac{\partial^{n+m} w(s,t)}{\partial s^n \partial t^m}\right| \leq C\varepsilon^{-n}\exp\left(-\beta(1-s)/\varepsilon\right), \quad (s,t) \in \Omega. \tag{10}$$

4 Numerical schemes

We are going to develop the numerical scheme in this section as well. After discretizing the temporal derivative with implicit Euler's method, the spatial derivative is discretized using the midpoint upwind approach by employing Shishkin mesh and obtaining the system of linear equations. This equation is then solved using any classical methods.

4.1 Temporal semi-discretization

We first partition the temporal domain $[0,\mathfrak{T}]$ to M_τ subintervals with uniform step size $\tau = \mathfrak{T}/M_\tau$. We chose M_τ such that for any positive integer $k \in (0, M_\tau)$, $\delta = k\tau$ must be a mesh point. The set Ω^{M_τ} represents all mesh points in the temporal direction. We then have $\Omega^{M_\tau} = \{t_0 = 0 < t_1 < t_2 < \cdots < t_k = \delta < t_{M_\tau - 1} < t_{M_\tau} = \mathfrak{T}\}$. We employ that $\Omega_\delta^{M_\tau}$ is the collection of all mesh points between zero and $-\delta$; that is, $\Omega_\delta^{M_\tau} = \{t_{-k} = -\delta < t_{-k+1} <$

$\cdots < t_{-1} < t_0 = 0\}$.

Consider the exact solution $w(s,t_{j+1})$ at $(j+1)^{th}$ mesh point and denote the approximation solution by $W^{j+1}(s)$. Let $z(s,t_{j+1}) = \frac{\partial^\gamma W(s,t_{j+1})}{\partial t^\gamma}$. According to Definition 4, then

$$\begin{aligned}
z(s,t_{j+1}) &= \frac{\partial^\gamma W(s,t_{j+1})}{\partial t^\gamma} \\
&= \frac{L(\gamma)}{1-\gamma}\int_0^t \frac{W(s,\xi)}{\partial\xi}\exp\left[-\gamma\frac{t_{j+1}-\xi}{1-\gamma}\right]d\xi \\
&= \frac{L(\gamma)}{1-\gamma}\sum_{i=0}^{j}\int_{i\tau}^{(i+1)\tau}\frac{W(s,\xi)}{\partial\xi}\exp\left(-\gamma\frac{t_{j+1}-\xi}{1-\gamma}\right)d\xi \\
&= \frac{L(\gamma)}{1-\gamma}\sum_{i=0}^{j}\frac{(W(s,t_{i+1})-W(s,t_i))}{\tau}\int_{(j-i)\tau}^{(j-i+1)\tau}\exp\left(-\gamma\frac{t_{j+1}-\xi}{1-\gamma}\right)d\xi \\
&\quad + \mathcal{R}_\tau \\
&= \frac{L(\gamma)}{1-\gamma}\sum_{i=0}^{j}\frac{(W(s,t_{j-i+1})-W(s,t_{j-i}))}{\tau} \\
&\quad \int_{(i)\tau}^{(i+1)\tau}\exp\left(-\gamma\frac{t_{j+1}-\xi}{1-\gamma}\right)d\xi + \mathcal{R}_\tau \\
&= \eta\Bigg[(W(s,t_{j+1})-W(s,t_j)) \\
&\quad + \sum_{i=1}^{j}(W(s,t_{j-i+1})-W(s,t_{j-i}))\exp\left(-\frac{\gamma\tau}{1-\gamma}i\right)\Bigg] + \mathcal{R}_\tau.
\end{aligned}$$

Let us consider $L(\gamma) = 1$ the normalization functions such that $L(0) = L(1) = 1$. Then

$$\eta = \frac{\exp\left(\frac{-\gamma\tau}{1-\tau}\right)-1}{\gamma\tau},$$

$$\mathcal{R}_\tau = \frac{O(\tau)}{1-\gamma}\int_0^{t_{j+1}}\exp\left(-\gamma\frac{t_{j+1}-\xi}{1-\gamma}\right)d\xi \quad \text{is the truncation error.}$$

Hence we obtain

$$\begin{aligned}
z(s,t_{j+1}) =& \eta\left(W(s,t_{j+1})-W(s,t_j)\right) \\
&+ \eta\sum_{i=1}^{j}(W(s,t_{j-i+1})-W(s,t_{j-i}))\exp\left(-\frac{\gamma\tau}{1-\gamma}i\right) + \mathcal{R}_\tau.
\end{aligned} \tag{11}$$

Substituting (11) into (1) on Ω^{M_τ}, we get

$$z(s,t_{j+1}) - \varepsilon\frac{\partial^2 W^{j+1}(s)}{\partial s^2} + a(s)\frac{\partial W^{j+1}(s)}{\partial s} + b^{j+1}(s)W^{j+1}(s) = -c^{j+1}(s)W^{j-k+1}(s) + f^{j+1}(s).$$

Once the expressions are rearranged and the operator form has been put in, we get

$$\tilde{\mathfrak{L}}W^{j+1}(s) = -\varepsilon\frac{\partial^2 W^{j+1}(s)}{\partial s^2} + a(s)\frac{\partial W^{j+1}(s)}{\partial s} + \nu^{j+1}(s)W^{j+1}(s) = F^j(s), \tag{12}$$

for $j = 1, 2, \ldots, M_\tau$ with

$$\begin{cases} w(s,t) = \varphi_b(s,t_j), & \text{for}(s,t) \in [0,1]\times[-\delta,0], \\ w(0,t_j) = \varphi_l(t_j), w(1,t_j) = \varphi_r(t_j), & \text{for } \ t \in (0,\mathfrak{T}), \end{cases} \tag{13}$$

where

$$\nu(s,t_{j+1}) = b^{j+1}(s) + \eta,$$

$$F^{j+1}(s) = \begin{cases} -c^{j+1}(s)\varphi_b(s,t_{j-k+1}) + f(s,t_{j+1}) \\ +\eta\sum_{i=1}^{j}\left(W(s,t_{j-i+1}) - W(s,t_{j-i})\right)\exp\left(-\frac{\gamma\tau}{1-\gamma}i\right) \\ +\eta W(s,t_j), & \text{for } \ j = 1,2,\ldots,k, \\ -c^{j+1}(s)W^{j-k+1}(s) + f^{j+1}(s) \\ +\eta\sum_{i=1}^{j}\left(W(s,t_{j-i+1}) - W(s,t_{j-i})\right)\exp\left(-\frac{\gamma\tau}{1-\gamma}i\right) \\ +\eta W(s,t_j), & \text{for } \ j = k+1,k+2,\ldots,M_\tau. \end{cases}$$

After some rearrangement of (12) we obtain

$$\left(1 + \alpha_0\mathfrak{L}^*_{\varepsilon,\delta}\right)W^{j+1}(x) = F^{j+1}(s), \tag{14}$$

where

$$\alpha_0 = \frac{\gamma\tau}{\exp\left(\frac{-\gamma\tau}{1-\gamma}\right) - 1},$$

$$\mathfrak{L}^*_{\varepsilon,\delta} = -\varepsilon\frac{\partial^2}{\partial s^2} + a(s)\frac{\partial}{\partial s} + b^{j+1}(s)$$

$$F^{j+1}(s)=\begin{cases}-\alpha_0 b^{j+1}(s)\varphi_b(s,t_{j-k+1})+\alpha_0 fj+1(s)\\ +\varphi_b(s,t_j)+\sum_{i=1}^{j}\left(W(s,t_{j-i+1})-W(s,t_{j-i})\right)\exp\left(-\frac{\gamma\tau}{1-\gamma}i\right)\\ +W(s,t_j), \qquad\qquad \text{for } \ j=1,2,\ldots,k,\\ -\alpha_0 s^{j+1}(s)W^{j-k+1}(s)+\alpha_0 fj+1(s)\\ +\varphi_b(x,t_j)+\sum_{i=1}^{j}\left(W(s,t_{j-i+1})-W(s,t_{j-i})\right)\exp\left(-\frac{\gamma\tau}{1-\gamma}i\right)\\ +W(s,t_j), \qquad\qquad \text{for } \ j=k+1,k+2,\ldots,M_\tau.\end{cases}$$

Lemma 5 (Semi-discrete maximum principle)**.** Let $\psi(s,t_{j+1})$ be a smooth function such that $\psi(0,t_{j+1})\geq 0$ and, $\psi(1,t_{j+1})\geq 0$, for all $(s,t_{j+1})\in\Lambda=\{0\}\times(0,\mathbb{T}]\cup\{1\}\times(0,\mathbb{T}]\cup[0,1]\times[-\delta,0]$. Then $(1+\alpha_0\mathfrak{L}^*_{\varepsilon,\delta})\psi(s,t_{j+1})\geq 0$ in Ω implies that $\psi(s,t_{j+1})\geq 0$, for all $(s,t_{j+1})\in\Omega$.

Proof. Suppose there exists $(\iota,t_{j+1})\in\bar{\Omega}$ with

$$\psi(\iota,t_{j+1})=\min_{(s,t_{j+1})\in\bar{\Omega}}\psi(s,t_{j+1}), \quad \text{and} \quad \psi(\iota,t_{j+1})<0.$$

Then we have

$$(\iota,t_{j+1})\notin\{(0,t_{j+1}),(1,t_{j+1})\} \quad \text{and} \quad \psi_s(\iota,t_{j+1})=0,\psi_{ss}(\iota,t_{j+1})>0.$$

Applying the operator $\mathfrak{L}^*_{\varepsilon,\delta}$ on $\psi(s,t_{j+1})$, we get

$$\begin{aligned}(1+\alpha_0\mathfrak{L}^*_{\varepsilon,\delta})\psi(\iota,t_{j+1})=&\psi(\iota,t_{j+1})+\alpha_0(-\varepsilon\psi_{xx}(\iota,t_{j+1})+a(\iota)\varphi_s(\iota,t_{j+1})\\ &+b(\iota,t_{j+1})\psi(\iota,t_{j+1})).\end{aligned}$$

The function ψ has a minimum at (ι,t_{j+1}), resulting in $\psi_s=0$, $\psi_{ss}\geq 0$, and $r(\iota,t_{j+1})\geq 0$ for $(\iota,t_{j+1})\in\Omega$. Therefore, we have

$$(1+\alpha_0\mathfrak{L}^*_{\varepsilon,\delta})\psi(\iota,t_{j+1})<0,$$

which contradicts our assumption of $(1+\mathfrak{L}^*_{\varepsilon,\delta})\psi(s,t_{j+1})$ in Ω.
Therefore, we conclude that $\psi(s,t_{j+1})\geq 0$, for all $(s,t_{j+1})\in\bar{\Omega}$.
Hence from the above, we prove that the operator $(1+\alpha_0\mathfrak{L}^*_{\varepsilon,\delta})$ satisfies the maximum principle and consequently

$$\left\|(1+\alpha_0\mathfrak{L}^*_{\varepsilon,\delta})^{-1}\right\|\leq\frac{1}{1+\theta\tau}. \tag{15}$$

□

Lemma 6 (Truncation error)**.** The local truncation error corresponding to the semi-discretized problem (13) satisfies

$$\left|\mathcal{R}_\tau^{j+1}\right| \leq C\tau. \tag{16}$$

Proof. From semi-discretized problem, we have

$$\begin{aligned}
\mathcal{R}_\tau^{j+1} &= \frac{O(\tau)}{1-\gamma}\int_0^{t_{j+1}} \exp\left(-\gamma\frac{t_{j+1}-\xi}{1-\gamma}\right)d\xi \\
&= \frac{O(\tau)}{1-\gamma}\int_0^{(j+1)\tau} \exp\left(-\gamma\frac{(j+1)\tau-\xi}{1-\gamma}\right)d\xi \\
&= \frac{O(\tau)\gamma}{(1-\gamma)^2}\left(\exp\left(-\gamma\frac{(j+1)\tau}{1-\gamma}\right)-\exp\left(\frac{-\gamma}{1-\gamma}\right)\right) \\
&\leq \frac{\gamma}{(1-\gamma)^2}\left(\exp\left(-\gamma\frac{j+1}{1-\gamma}\right)-\exp\left(\frac{-\gamma}{1-\gamma}\right)\right)\tau \\
&\leq C\tau,
\end{aligned}$$

since $\exp\left(-\gamma\frac{(j+1)\tau}{1-\gamma}\right) \leq \exp\left(-\gamma\frac{j+1}{1-\gamma}\right)$ and

$$C = \frac{\gamma}{(1-\gamma)^2}\left(\exp\left(-\gamma\frac{j+1}{1-\gamma}\right)-\exp\left(\frac{-\gamma}{1-\gamma}\right)\right).$$

Therefore, we obtain

$$\left|\mathcal{R}_\tau^{j+1}\right| \leq C\tau.$$

□

Lemma 7 (Error bound)**.** The global error estimation at t_{j+1} satisfies

$$\|E_{j+1}\| \leq C\tau.$$

Proof. Since the function $y(x, t_{j+1})$ satisfies

$$(1+\alpha_0\mathfrak{L}_{\varepsilon,\delta}^*)y(x,t_{j+1}) = F^{j+1}(x), \tag{17}$$

also the solution of the continuous problem (1)–(2) is smooth enough, then we have

$$\begin{aligned}
F^{j+1}(s) &= (1+\alpha_0\mathfrak{L}_{\varepsilon,\delta}^*)W(s,t_{j+1}) + \mathcal{R}_\tau^{j+1} \\
&= (1+\alpha_0\mathfrak{L}_{\varepsilon,\delta}^*)W(s,t_{j+1}) + C\tau
\end{aligned}$$

$$\Longrightarrow F^{j+1}(s) = (1 + \alpha_0 \mathfrak{L}^*_{\varepsilon,\delta}) W(s, t_{j+1}) + C\tau. \tag{18}$$

From (17)–(18), the error corresponding to (14) satisfies the following problem

$$(1 + \alpha_0 \mathfrak{L}^*_{\varepsilon,\delta}) E_{j+1} = C\tau$$
$$\Longrightarrow E_{j+1} = (1 + \alpha_0 \mathfrak{L}^*_{\varepsilon,\delta})^{-1} \tau$$

$$\|E_{j+1}\| \leq \frac{1}{1 + \theta\tau} C\tau.$$

Hence, we obtain the result

$$\|E_{j+1}\| \leq C\tau.$$

□

Theorem 1. The semi-discretize solution $W(s, t_{j+1})$ and its derivatives meet the following bounds:

$$\left| \frac{d^i W(s, t_{j+1})}{ds^i} \right| \leq C(1 + \varepsilon^{-i} \exp(-\beta(1 - s)/\varepsilon)), \quad \text{for} \quad i = 0, 1, 2, 3, 4.$$

Proof. For the proof, refer [8]. □

We can rewrite (12) as operator form

$$\tilde{\mathfrak{L}}^\tau_\varepsilon W^{j+1}(s) = F^{j+1}(s), \tag{19}$$

where $\tilde{\mathfrak{L}}^\tau_\varepsilon W^{j+1}(s) = -\varepsilon \frac{\partial^2 W^{j+1}(s)}{\partial s^2} + a(s) \frac{\partial W^{j+1}(s)}{\partial s} + \nu(s) W^{j+1}(s)$ and

$$F^j(x) = \begin{cases} -s^{j+1}(s)\varphi_b(s, t_{j-k+1}) + f(s, t_{j+1}) \\ +\sigma B_j \varphi_b(s, t_j) + \sigma \sum_{i=1}^{j} B_i \left(W(s, t_{j-i+1}) \right. \\ \left. -W(s, t_{j-i}) \right), \qquad \text{for } j = 1, 2, \ldots, k, \\ -s^{j+1}(s) W^{j-k+1}(s) + f^{j+1}(s) \\ +\sigma \psi_b(s, t_j) + \sigma \sum_{i=1}^{j} B_i \left(W(s, t_{j-i+1}) \right. \\ \left. -W(s, t_{j-i}) \right), \qquad \text{for } j = k+1, k+2, \ldots, M_\tau. \end{cases}$$

Lemma 8. [9] Consider the regular V^{j+1} and singular U^{j+1} components of W^{j+1} and their derivatives, which holds the following bounds:

$$\left|\frac{\partial^n V^{j+1}(x)}{\partial x^n}\right| \leq C\left(1+\varepsilon^{4-n}\right), \tag{20}$$

$$\left|\frac{\partial^n U^{j+1}(s)}{\partial s^n}\right| \leq C\varepsilon^{-n}\exp\left(-\alpha(1-s)/\varepsilon\right), \qquad n=0,1,\ldots,4. \tag{21}$$

4.2 Spatial discretization

4.2.1 Mesh generation

To address the semi-discretized problem (12), we used a piecewise-uniform Shishkin mesh to partition the space domain. This ensures that the boundary layer region had more mesh points than the outer region. The domain $[0,1]$ is separated into two subdomains, $[0,1-\sigma]$ and $(1-\sigma,1]$, where σ is given as

$$\sigma = \min\{0.5, \sigma_0\varepsilon\ln N\},$$

with boundary point $1-\sigma$, whereas $\sigma_0 \leq 1/\beta$ and N is the number of subintervals. The mesh sizes in the inner and outer boundary layer are

$$h_i = \begin{cases} \frac{2(1-\sigma)}{N}, & i=0,1,\ldots,\frac{N}{2}, \\ \frac{2\sigma}{N}, & i=\frac{N}{2}+1,\ldots,N. \end{cases}$$

The mesh points have been defined by

$$x_i = \begin{cases} i\frac{2(1-\sigma)}{N}, & i=0,1,\ldots,\frac{N}{2}, \\ 1-\sigma+(i-\frac{N}{2})\frac{2\sigma}{N}, & i=\frac{N}{2}+1,\ldots,N. \end{cases}$$

The set Ω^N represents all mesh points along the spatial direction. Hence, we have

$$\Omega^N = \{x_0 = 0 < x_1 < \cdots < x_{N-1} < x_N = 1\}.$$

The set Ω^N is the set that includes all mesh points along the spatial direction with equal step size $h = 1/N$ over $\sigma = 1/2$.

In the next section, we derive stable finite difference method.

4.2.2 Upwind numerical scheme

We utilize a midpoint upwind finite difference approach on the semi-discrete scheme (12) along the spatial direction. The difference operators with $\hat{h}_i = h_i + h_{i+1}$ are given as

$$\begin{aligned} D_s^- W_i^{j+1} &= \frac{W_i^{j+1} - W_{i-1}^{j+1}}{h_i}, \quad D_s^+ W_i^{j+1} = \frac{W_{i+1}^{j+1} - W_i^{j+1}}{h_{i+1}}, \\ D_s^0 W_i^{j+1} &= \frac{W_{i+1}^{j+1} - W_{i-1}^{j+1}}{\hat{h}_i}, \quad \delta_s^2 W_i^{j+1} = \frac{2}{\hat{h}_i}\left(D^+ W_i^{j+1} - D^- W_i^{j+1}\right). \end{aligned} \tag{22}$$

Additionally, we define $W_{i-1/2}^{j+1} = \frac{W_i^{j+1} + W_{i-1}^{j+1}}{2}$. We similarly define other terms.

Therefore using these difference operators, we derive the complete finite difference scheme:

$$\begin{cases} W_0^{j+1} = \varphi_l(0, t_{j+1}), \\ \tilde{\mathfrak{L}}_{mpu}^{\tau,h_i} W_{i-1/2}^{j+1} = F_{i-1/2}^{j+1}, \quad i = 1, 2, \ldots, N, \\ W_N^{j+1} = \varphi_r(1, t_{j+1}), \end{cases} \tag{23}$$

where

$$\begin{aligned} \tilde{\mathfrak{L}}_{mpu}^{\tau,h_i} &= -\varepsilon \delta_s^2 + a_{i-1/2} D_s^- + \nu_{i-1/2}, \\ F_{i-1/2}^{j+1} &= -c_{i-1/2}^{j+1} W_{i-1/2}^{j-k+1} + f_{i-1/2}^{j+1} \\ &\quad + \eta \sum_{m=1}^{j} \left(W_{i-1/2}^{j-m+1} - W_{i-1/2}^{j-m}\right) \exp\left(-\frac{\gamma\tau}{1-\gamma} m\right) + \eta W_{i-1/2}^{j}. \end{aligned}$$

Through the rearrangement of equation (23), we deduce the subsequent system of equations:

$$\Upsilon_i^- W_{i-1}^{j+1} + \Upsilon_i^0 W_i^{j+1} + \Upsilon_{i+1}^+ W_{i-1}^{j+1} = F_{i-1/2}^{j+1}, \qquad i = 1, 2, \ldots, N, \tag{24}$$

$$\begin{cases} \Upsilon_i^- = -\frac{2\varepsilon}{h_i \hat{h}_i} - \frac{q_{i-1/2}}{h_i} + \frac{\nu_{i-1/2}^{j+1}}{2}, \\ \Upsilon_i^0 = \frac{2\varepsilon}{h_i h_{i+1}} + \frac{q_{i-1/2}}{h_i} + \frac{\nu_{i-1/2}^{j+1}}{2}, \\ \Upsilon_i^+ = -\frac{2\varepsilon}{h_{i+1} \hat{h}_i}. \end{cases}$$

5 Convergence analysis

This section discusses the stability of the discretized scheme (24). To determine the ε-uniform error estimate, the truncation error is used. The stability of the developed scheme can be studied using the following lemma.

Lemma 9 (Discrete maximum principle)**.** Let φ_i^j be any function satisfying $\varphi_0 \geq 0$, $\varphi_{N+1} \geq 0$. Then $\tilde{\mathfrak{L}}_{mpu}^{\tau,h_i}\Phi_i^{j+1} \geq 0$, for all $i = 1, 2, 3, \ldots, N$, implies that $\varphi_i^j \geq 0$ for all $i = 1, 2, 3, \ldots, N$.

Proof. This follows the same arguments as in Lemma 5. □

Lemma 10. Consider the difference operator of (24) $\tilde{\mathfrak{L}}_{mpu}^{\tau,h_i}W_i^{j+1}, i = 1, 2, \ldots.N-1$, with boundaries W_0^{j+1} and W_N^{j+1} has a solution. If $\tilde{\mathfrak{L}}_{mpu}^{\tau,h_i}W_i^{j+1} \leq \tilde{\mathfrak{L}}_{mpu}^{\tau,h_i}Z_i^{j+1}$, $W_0^{j+1} \leq Z_0^{j+1}$ and $W_N^{j+1} \leq Z_N^{j+1}$, then $W_i^{j+1} \leq Z_i^{j+1}, i = 1, 2, \ldots, N-1$.

Proof. The coefficient matrix for the operator $\tilde{\mathfrak{L}}_{\varepsilon}^{h,\tau}$ has a size of $(N_h+1)(N_h+1)$ with its constituents, for $i = 1, 2, \ldots, N_h - 1$, are

$$\Upsilon_i^- = -\frac{2\varepsilon}{h_i\hat{h}_i} - \frac{q_{i-1/2}}{h_i} + \frac{\nu_{i-1/2}^{j+1}}{2} < 0, \quad \text{since} \quad \text{all} \quad \text{terms} \quad \text{are positive},$$

$$\Upsilon_i^0 = \frac{2\varepsilon}{h_i h_{i+1}} + \frac{q_{i-1/2}}{h_i} + \frac{\nu_{i-1/2}^{j+1}}{2} > 0, \quad \text{since} \quad \text{all} \quad \text{terms} \quad \text{are positive},$$

$$\Upsilon_i^+ = -\frac{2\varepsilon}{h_{i+1}\hat{h}_i} < 0, \quad \text{since} \quad \text{all} \quad \text{terms} \quad \text{are positive}.$$

The proposed method's coefficient matrix (24) for the differential equation (1)–(2) meets the properties of an M-matrix. This suggests that the inverse matrix exists and is not negative. This ensures the existence and uniqueness of the discrete solution. A similar procedure was used to demonstrate the stability of a discrete scheme in [36, 24]. □

A direct consequence of Lemma 10 is the discrete stability result as follows.

Lemma 11 (The discrete stability result)**.** If W_i^{j+1} is the solution of the fully discretized equation corresponding to the original problem in (1), such that $W_0^{j+1} = W_N^{j+1} = 0$, then the following inequality is satisfied:

$$\left|W_i^{j+1}\right| \leq \left\|\tilde{\mathfrak{L}}_{mpu}^{\tau,h_i} W_i^{j+1}\right\| + \max_{0\leq i,j\leq N,M}\{|\varphi l|, |\varphi r|\}.$$

Proof. Consider two barrier functions

$$\prod^{\pm} = \zeta \pm W_i^{j+1}, \quad \text{where} \quad \zeta = \left\|\tilde{\mathfrak{L}}_{mpu}^{\tau,h_i} W_i^{j+1}\right\| + \max_{1\leq i,j\leq N,M}\{|\varphi_l|, |\varphi_r|\}$$

At the boundaries
$\prod_0^{\pm} = \zeta \pm w(0,t_j) = \left\|\tilde{\mathfrak{L}}_{mpu}^{\tau,h_i} W_i^{j+1}\right\| + \max_{1\leq j\leq M}\{|\varphi_l|, |\varphi_r|\} \pm \varphi_l \geq 0$ and
$\prod_N^{\pm} = \zeta \pm w(1,t_j) = \left\|\tilde{\mathfrak{L}}_{mpu}^{\tau,h_i} W_i^{j+1}\right\| + \max_{1\leq j\leq M}\{|\varphi_l|, |\varphi_r|\} \pm \varphi_r \geq 0.$
Using the operator $\tilde{\mathfrak{L}}_{mpu}^{\tau,h_i}$ on the barrier function, we have

$$\begin{aligned}
\tilde{\mathfrak{L}}_{mpu}^{\tau,h_i} \prod_i^{\pm} &= \left(-\varepsilon\delta_s^2 + a_{i-1/2}D_s^- + \nu_{i-1/2}\right)\left(\zeta \pm W_i^{j+1}\right) \\
&= -\varepsilon\delta_s^2\left(\zeta \pm W_i^{j+1}\right) + a_{i-1/2}D_s^-\left(\zeta \pm W_i^{j+1}\right) + \nu_{i-1/2}\left(\zeta \pm W_i^{j+1}\right) \\
&\geq \left\|\tilde{\mathfrak{L}}_{\varepsilon}^{h,\tau} W_i^{j+1}\right\| + \max_{1\leq i,j\leq N,M_\tau}\{|\varphi_l|, |\varphi_r|\} \pm W_i^{j+1} \\
&\geq 0.
\end{aligned}$$

By using the maximum principle, Lemma 9, we get

$$\tilde{\mathfrak{L}}_{mpu}^{\tau,h_i} \prod^{\pm} \geq 0 \quad \Longrightarrow \left|W_i^{j+1}\right| \leq \left\|\tilde{\mathfrak{L}}_{mpu}^{\tau,h_i} W_i^{j+1}\right\| + \max_{0\leq i,j\leq NM_\tau}\{|\varphi l| + |\varphi r|\}.$$

□

Lemma 12. [31] Consider the mesh function Λ_i, for $i = 0, 1, \ldots, N$ defined by

$$\Lambda_i^{j+1} = \prod_{l=1}^{i}\left(1 + \frac{\alpha h_l}{2\varepsilon}\right),$$

with the familiar convection that if $i = 0$, then $\Lambda_0^{j+1} = 1$. Then, for $i = 1, 2, \ldots, N-1$, a positive constant C exists such that

$$\tilde{\mathfrak{L}}_{mpu}^{\tau,h_i}\Lambda_i^{j+1} \geq \frac{C}{\max(\varepsilon, h_i)}\Lambda_i^{j+1}.$$

Theorem 2. Let $w(s_i, t_j)$ represent the exact solution for the problem (1) and let W_i represent the full discretization solution for problem (19). The error estimate is then provided by

$$|W_i - w(s_i, t_j)| \leq CN^{-1}(\ln N)^2.$$

Proof. The discrete problem's solution, W_i, can be divided into regular V_i and singular U_i components.
Thus

$$W_i^{j+1} = V_i^{j+1} + U_i^{j+1}.$$

Moreover, V_i and U_i represent the solutions to the following problems, respectively:

$$\tilde{\mathfrak{L}}_{mpu}^{\tau,h_i} V_i = F_{i-1/2}, V_i(0) = v(0), V_i(1) = v(1) \text{(nonhomogeneous problem)}$$

$$\tilde{\mathfrak{L}}_{mpu}^{\tau,h_i} U_i = 0, U_i(0) = u(0), U_i(1) = u(1) \quad \text{(homogeneous problem)}$$

Consider $W_i^{j+1} = W_i, V_i^{j+1} = V_i$, and $U_i^{j+1} = U_i$.

The error can be expressed as

$$W_i - w(x_i) = (V_i + U_i) - (v(x_i) + u(x_i)),$$

$$W_i - w(x_i) = (V_i - v(x_i)) + (U_i - u(x_i)). \tag{25}$$

Using the triangle inequality, the error can be estimated as

$$\|W_i - w(s_i)\| \leq \|V_i - v(s_i)\| + \|U_i - u(s_i)\|.$$

Next, we need to estimate the errors in the regular and singular components individually.

The following classical reasoning can be used to calculate the error estimate for a regular component. From the differential and difference equations, we get

$$\begin{aligned}
\tilde{\mathfrak{L}}_{mpu}^{\tau,h_i}(V_i - v(s_i)) &= \tilde{\mathfrak{L}}_{mpu}^{\tau,h_i} V_i - \tilde{\mathfrak{L}}_{mpu}^{\tau,h_i} v(s_i) \\
&= F_i - \tilde{\mathfrak{L}}_{mpu}^{\tau,h_i} v(s_i) \\
&= \left(\tilde{\mathfrak{L}} - \tilde{\mathfrak{L}}_{mpu}^{\tau,h_i}\right) v(s_i) \\
&= -\varepsilon \left(\frac{d^2}{dx^2} - \delta^2\right) v(s_i) + a \left(\frac{d}{ds} - D^-\right) v(s_i).
\end{aligned}$$

By using the estimate in [22], we get

$$\begin{aligned}\left|\tilde{\mathfrak{L}}_{mpu}^{\tau,h_i}\left(V_i - v(x_i)\right)\right| &\leq \frac{1}{4}\left(x_{i+1} - x_{i-1}\right)|v|_3 + \frac{1}{2}\left(x_i - x_{i-1}\right)|v|_2 \\ &\leq \frac{1}{4}\left(x_{i+1} - x_{i-1}\right)|v|_3 + \frac{1}{2}\left(x_{i+1} - x_{i-1}\right)|v|_2 \\ &\qquad\qquad \text{since} \quad x_i - x_{i-1} \leq x_{i+1} - x_{i-1}, \\ &\leq C\left(x_{i+1} - x_{i-1}\right)\left(|v|_3 + |v|_2\right).\end{aligned}$$

Therefore, we obtain

$$\left|\tilde{\mathfrak{L}}_{mpu}^{\tau,h_i}\left(V_i - v(s_i)\right)\right| \leq C\left(s_{i+1} - s_{i-1}\right)\left(|v|_3 + |v|_2\right). \tag{26}$$

Indeed $s_{i+1} - s_{i-1} \leq 2N^{-1}$, for all $i, 0 \leq i \leq N-1$ and applying the discrete stability lemma for the regular component, v satisfies the following bound of the derivatives:

$$\left|v^{(k)}(s)\right| \leq C\left(1 + \varepsilon^{-\frac{(k-2)}{2}}\right), \qquad 0 \leq k \leq 4. \tag{27}$$

Then from (27) we obtain

$$|v|_2 = |v''| \leq C, \quad \text{and} \quad |v|_3 = |v'''| \leq C(1 + \varepsilon^{-\frac{1}{2}}). \tag{28}$$

By substituting (28) into (26), for the estimates of the derivatives of v, we have

$$\left|\tilde{\mathfrak{L}}_{mpu}^{\tau,h_i}\left(V_i - v(s_i)\right)\right| \leq CN^{-1}.$$

Next, we apply maximum principle result for the operator $\tilde{\mathfrak{L}}_{mpu}^{\tau,h_i}$ to the function $V_i - v(x)$. Then we obtain

$$|(V_i - v(s))| \leq CN^{-1}. \tag{29}$$

The error estimate regarding the singular component $U_i - u(x_i)$ is determined by the transition parameter value, which is either $\sigma = 1/2$ or $\sigma = \sigma_0 \varepsilon \ln N$.

Case-I: For $\sigma = \frac{1}{2}$, the grids are equal and $\varepsilon\sigma_0 \ln N \geqslant \frac{1}{2}$, resulting in

$$s_{i+1} - s_{i-1} = 2N^{-1} \quad \text{and} \quad \varepsilon^{-1} \leq C \ln N. \tag{30}$$

The classical argument, which was used earlier to estimate the regular argument, concludes

$$\left|\tilde{\mathfrak{L}}_{mpu}^{\tau,h_i}(U_i - u(s_i))\right| \leq C\left(s_{i+1} - s_{i-1}\right)\left(|u|_3 + |u|_2\right).$$

We use a similar fashion with the regular component. Also, $s_{i+1} - s_{i-1} = 2N^{-1}$ and $\varepsilon^{-1} \leq C \ln N$. Then we have

$$\left|\tilde{\mathfrak{L}}_{mpu}^{\tau,h_i}(U_i - u(s_i))\right| \leq C\varepsilon^{-2}N^{-1}.$$

Therefore, we obtain

$$\left|\tilde{\mathfrak{L}}_{mpu}^{\tau,h_i}(U_i - u(s_i))\right| leqC\varepsilon^{-2}N^{-1}. \tag{31}$$

Substituting (30) into (31), then we get

$$\left|\tilde{\mathfrak{L}}_{mpu}^{\tau,h_i}(U_i - u(s_i))\right| \leq CN^{-1}(\ln N)^2.$$

An application to ε-uniform stability result for the operator $\tilde{\mathfrak{L}}_{mpu}^{\tau,h_i}$ to the function $U_i - u(s_i)$ then gives

$$|U_i - u(s_i)| \leq CN^{-1}(\ln N)^2. \tag{32}$$

Case-II: If $\sigma = \varepsilon\sigma_0 \ln N < \frac{1}{2}$, the mesh is piece-wise uniform, with the mesh spacing $\frac{2(1-\sigma)}{N}$ in the subinterval $[0, 1-\sigma]$ and $\frac{2\sigma}{N}$ in the subinterval $[1-\sigma, 1]$, then we estimate the error in $[0, 1-\sigma]$ and $[1-\sigma, 1]$ individually. In the subinterval $[0, 1-\sigma]$ without boundary layer both U_i and $u(s_i)$ are small and since by triangle inequality $|U_i - u(s_i)| \leq |U_i| + |u(x_i)|$, it helps to bound U_i and u individually.
We assumed that $\sigma = \sigma_0\varepsilon \ln N (> 2\varepsilon \ln N/\alpha)$, which gives $-\alpha\sigma/\varepsilon < \ln N^{-2}$. From lemma 8, we have

$$\begin{aligned} |U_i| &\leq Ce^{-\alpha\sigma/\varepsilon} \\ &\leq Ce^{-\alpha(\frac{\varepsilon \ln N}{\alpha})/\varepsilon} \\ &\leq Ce^{-\ln N} \\ &\leq CN^{-1}, \end{aligned}$$

$$|U_i| \leq CN^{-1}. \tag{33}$$

Next, we need to show $|U_i| \leq CN^{-1}$ for a suitable constant C.

Let $\Lambda_i^{j+1} = \Lambda_i$. From the Taylor series expansion $e^s \geq 1+s$, then for the mesh function Λ_i,

$$\begin{aligned}\Lambda_N &= \prod_{l=1}^{N}\left(1+\frac{\alpha h_l}{2\varepsilon}\right)\\ &= \prod_{l=1}^{i}\left(1+\frac{\alpha h_l}{2\varepsilon}\right)\prod_{l=i+1}^{N}\left(1+\frac{\alpha h_l}{2\varepsilon}\right)\\ &= \Lambda_i\prod_{l=i+1}^{N}\left(1+\frac{\alpha h_l}{2\varepsilon}\right),\\ \Lambda_i/\Lambda_N &= \prod_{l=i+1}^{N}\left(1+\frac{\alpha h_l}{2\varepsilon}\right)^{-1} \geq \prod_{l=i+1}^{N}\exp\left(-\frac{\alpha h_l}{2\varepsilon}\right) = \exp\left(-\frac{\alpha(1-x_i)}{2\varepsilon}\right).\end{aligned}$$

Let $\hat{\Lambda}_i = C\Lambda_i/\Lambda_N$ for $i = 0, 1, \ldots, N$. Hence by using the definition of U_i and Lemma 12,

$$\tilde{\mathfrak{L}}_{mpu}^{\tau,h_i}\hat{\Lambda}_0 = \left(\frac{C}{\Lambda_N}\right)\tilde{\mathfrak{L}}_{mpu}^{\tau,h_i}\Lambda_i \geq \left(\frac{C}{\Lambda_N}\right)\frac{\Lambda_i}{\max\{\varepsilon,h_i\}} \geq 0 = \left|\tilde{\mathfrak{L}}_{mpu}^{\tau,h_i}U_N\right|,$$

$$\tilde{\mathfrak{L}}_{mpu}^{\tau,h_i}\hat{\Lambda}_0 \geq 0. \tag{34}$$

For a suitably large value of C, we get that

$$\hat{\Lambda}_0 = \frac{C\Lambda_0}{\Lambda_N} \geq C\exp\left(\frac{-\alpha}{2\varepsilon}\right) \geq C\exp\left(\frac{-\alpha}{\varepsilon}\right) \geq |U_0|, \tag{35}$$

$$\hat{\Lambda}_0 = C \geq |U_N|. \tag{36}$$

Using (34)–(36), by the discrete comparison principle, Lemma 10, we obtain

$$|U_i| \leq \hat{\Lambda}_i = C\Lambda_i/\Lambda_N.$$

When $i = 0, 1, \ldots, N/2$,

$$\Lambda_i/\Lambda_N \leq \prod_{l=N/2+1}^{N}\left(1+\frac{\alpha(x_{i+1}-x_{i-1})}{2\varepsilon}\right)^{-1} = \left(1+2N^{-1}\ln N\right)^{-N/2}. \tag{37}$$

After some simplification and the Taylor series expansion, $\ln(1+s) > s - \frac{s^2}{2}, s > 0$, to the right end expression of (37), we get

$$|U_i| \leq CN^{-1}, \quad \text{for} \quad i = 0, 1, \ldots, N/2. \tag{38}$$

Combining (33) and (38), we obtain our result

$$|U_i| \leq CN^{-1}. \tag{39}$$

Triangle inequality results

$$|U_i - u(s_i)| \leq CN^{-1}, \quad \text{for} \quad 0 \leq i \leq N/2. \tag{40}$$

Next, we consider the subinterval $[1-\sigma, 1]$.

Using the classical argument, we get

$$\left|\tilde{\mathfrak{L}}^{\tau,h_i}_{mpu}\left(U_i - u(s_i)\right)\right| \leq C\varepsilon^{-2}(s_{i+1} - s_{i-1}), \quad \text{for} \quad N/2+1, N/2+2, \ldots, N-1.$$

For the second interval, the mesh spacing is $2\sigma/N$. Since $s_{i+1} - s_{i-1} = 4\sigma/N$, we obtain that

$$\left|\tilde{\mathfrak{L}}^{\tau,h_i}_{mpu}\left(U_i - u(s_i)\right)\right| \leq C\varepsilon^{-2}\sigma N^{-1}, \quad \text{for} \quad N/2+1, N/2+2, \ldots, N-1, \tag{41}$$

and

$$|U_N - u(1)| = 0.$$

Also, using the inequality (40), we obtain

$$\left|U_{N/2} - u(s_{N/2})\right| \leq CN^{-1}. \tag{42}$$

Now, we introduce the barrier function, with the suitable choices of C_1 and C_2 as

$$\xi_i = (s_i - (1-\sigma))C_1\varepsilon^{-2}\sigma N^{-1} + C_2 N^{-1},$$

and the mesh function

$$\chi_i^{\pm} = \xi_i \pm (u(s_i) - U_i), \quad N/2 \leq i \leq N.$$

Thus, we have

$$\begin{aligned}
\chi^{\pm}_{N/2} &= \xi_{N/2} \pm (u(s_{N/2}) - U_{N/2}) \\
&\geq (s_{N/2} - (1-\sigma))C_1\varepsilon^{-2}\sigma N^{-1} + C_2 N^{-1} \pm (\mp CN^{-1}) \\
&\geq C_2 N^{-1} \pm (\mp CN^{-1}) \quad \text{since} \quad s_{N/2} = 1-\sigma
\end{aligned}$$

$$\geq (C_2 \mp C)N^{-1}.$$

Choose C_2 as $C_2 \mp C \geq 0$ and then

$$\chi_{N/2}^{\pm} \geq 0.$$

Next, we want to show that $\chi_N \pm \geq 0$. Therefore,

$$\begin{aligned}
\chi_N^{\pm} &= \xi_N \pm (u(s_N) - U_N) \\
&\geq (s_N - (1-\sigma))C_1\varepsilon^{-2}\sigma N^{-1} + C_2N^{-1} \\
&\geq C_1\sigma\sigma_0(\ln N)^2N^{-1} + C_2N^{-1} \\
&\geq 0.
\end{aligned}$$

Lastly, we need to show that $\tilde{\mathfrak{L}}_{mpu}^{\tau,h_i}\chi_i^{\pm} \geq 0$. Hence

$$\begin{aligned}
\tilde{\mathfrak{L}}_{mpu}^{\tau,h_i}\chi_i^{\pm} &= \tilde{\mathfrak{L}}_{mpu}^{\tau,h_i}\left[\xi_i \pm (u(s_i) - U_i)\right] \\
&= \tilde{\mathfrak{L}}_{mpu}^{\tau,h_i}\xi_i \pm \tilde{\mathfrak{L}}_{mpu}^{\tau,h_i}(u(s_i) - U_i) \\
&\geq \left(\beta + \frac{2}{\tau}\right)\left((s_i - (1-\sigma))C_1\varepsilon^{-2}\sigma N^{-1} + C_2N^{-1}\right) \\
&\quad \pm \tilde{\mathfrak{L}}_{mpu}^{\tau,h_i}(u(s_i) - U_i) \\
&\geq (s_i - (1-\sigma))C_1\varepsilon^{-2}\sigma N^{-1} + C_2N^{-1} + C_2N^{-1} \\
&\quad \pm (\mp C\varepsilon^{-2}\sigma N^{-1}), \quad \text{by (41)} \\
&\geq (s_i - \sigma)C_1\varepsilon^{-2}\sigma N^{-1} + C_2N^{-1} + C_2N^{-1} \pm (\mp C\varepsilon^{-2}\sigma N^{-1}) \\
&\geq ((s_i - \sigma)C_1 \mp C)\varepsilon^{-2}\sigma N^{-1} + C_2N^{-1} + C_2N^{-1} \\
&\geq 0, \quad \text{since} \quad (s_i - \sigma) \geq 0 \quad \text{then} \quad (s_i - \sigma)C_1 \mp C \geq 0.
\end{aligned}$$

Therefore by using the discrete maximum principle, we have

$$\chi_i^{\pm} \geq 0, \quad N/2 \leq i \leq N.$$

Thus we obtain the result

$$\left|u^{j+1}(s_i) - U_i^{j+1}\right| \leq CN^{-1}(\ln N)^2. \tag{43}$$

Then combining (32) and (43), we get

$$\left|u^{j+1}(s_i) - U_i^{j+1}\right| \leq CN^{-1}(\ln N)^2, \quad \text{for} \quad 0 \leq i \leq N. \tag{44}$$

Therefore, using (25) the inequalities in (29) and (44), gives

$$\left|(W_i^{j+1} - w(s_i, t_{j+1})\right| \leq CN^{-1}(\ln N)^2.$$

□

Theorem 3. If w and W are exact and approximation solution of the problem (1), respectively, then the following error bound holds:

$$\left|w(s_i, t_j) - W_i^{j+1}\right| \leq C\left(N^{-1}(\ln N)^2 + \tau\right). \tag{45}$$

Proof. By combining Lemma 7 and Theorem 2 we get our result. □

6 Numerical result

In this section, we present two numerical examples that illustrate the method's accuracy as well as the error analysis results. Separate tables show the error and convergence rates for each of these two instances of the test. This article will employ double mesh to determine the numerical solution's accuracy, as the exact answer is uncertain. The maximum point-wise absolute error is calculated as

$$E_\varepsilon^{N,M} = \max_{0\leq i,j\leq N,M} \left|W_{i,j}^{N,M} - W_{2i,2j}^{2N,2M}\right|,$$

where N and M represent the number of mesh points in spatial and temporal directions, respectively. The parameter for uniform error estimation is

$$e^{N,M} = \max_\varepsilon\{E_\varepsilon^{N,M}\}$$

. The method's rate of convergence is determined using the formula

$$RoC_\varepsilon^{N,M} = \log_2\left(\frac{E_\varepsilon^{N,M}}{E_\varepsilon^{2N,2M}}\right).$$

. The parameter uniform rate of convergence can be stated as

$$R^{N,M} = \max_\varepsilon\{RoC_\varepsilon^{N,M}\}$$

Example 1. Consider the time-fractional partial differential equation

$$D_t^{\gamma} y(s,t) - \varepsilon \frac{\partial^2 y(s,t)}{\partial s^2} + \left(2 - s^2\right) \frac{\partial y(s,t)}{\partial s} + ((s+1)(t+1))y(s,t)$$
$$= y(s,t-1) + 10t^2 \exp(-t)s(1-s),$$

on $(s,t) \in \Omega = (0,1) \times (0,\mathfrak{T}]$, with initial and boundary conditions $\varphi_b(s,t) = 0$, $\varphi_l(t) = 0$, and $\varphi_r(t) = 0$.

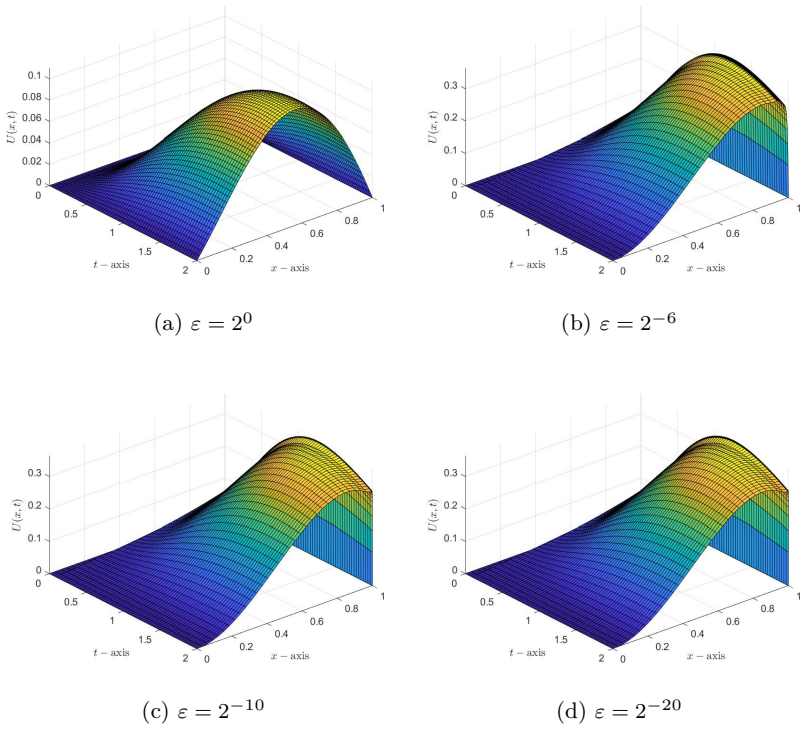

(a) $\varepsilon = 2^0$ (b) $\varepsilon = 2^{-6}$

(c) $\varepsilon = 2^{-10}$ (d) $\varepsilon = 2^{-20}$

Figure 1: A three-dimensional depiction of the numerical solution for Example 1 with various values of ε with $\gamma = 0.5$, $N_h = 32$, and $M_\tau = 40$.

Example 2. Consider the time-fractional partial differential equation

$$D_t^{\gamma} y(s,t) - \varepsilon \frac{\partial^2 y(s,t)}{\partial s^2} + \left(2 - s^2\right) \frac{\partial y(s,t)}{\partial s} + sy(s,t)$$
$$= y(s,t-1) + 10t^2 \exp(-t)s(1-s),$$

on $(s,t) \in \Omega = (0,1) \times (0,\mathfrak{T}]$, with initial and boundary conditions $\varphi_b(s,t) = 0$, $\varphi_l(t) = 0$, and $\varphi_r(t) = 0$.

Table 1: The absolute maximum error and rate of convergence for Example 1 for various values of ε, with fix $\gamma = 0.5$

$N_h = M_\tau \Rightarrow$	32	64	128	256	512
$\varepsilon = 1$	7.2009e-03	3.9138e-03	2.0434e-03	1.0436e-03	5.3354e-04
	0.8796	0.9376	0.9693	0.9679	-
$\varepsilon = 2^{-4}$	1.3920e-02	8.8730e-03	4.8151e-03	2.4093e-03	1.1793e-03
	0.6497	0.8819	0.9990	1.0307	-
$\varepsilon = 2^{-8}$	8.6296e-02	5.0505e-02	2.7245e-02	1.3603e-02	6.3990e-03
	0.7729	0.8904	1.0020	1.0881	-
$\varepsilon = 2^{-12}$	4.3419e-03	1.9191e-03	9.1791e-04	4.6674e-04	2.3530e-04
	1.1779	1.0640	0.9757	0.9881	-
$\varepsilon = 2^{-16}$	1.0750e-01	6.3792e-02	3.5339e-02	1.8579e-02	9.5447e-03
	0.7529	0.8521	0.9276	0.9609	-
$\varepsilon = 2^{-20}$	1.0772e-01	6.3935e-02	3.5424e-02	1.8631e-02	9.5791e-03
	0.7526	0.8519	0.9270	0.9597	-
$\varepsilon = 2^{-24}$	1.0773e-01	6.3940e-02	3.5427e-02	1.8633e-02	9.5802e-03
	0.7526	0.8519	0.9270	0.9597	-
$\varepsilon = 2^{-30}$	1.0773e-01	6.3940e-02	3.5427e-02	1.8633e-02	9.5803e-03
	0.7526	0.8519	0.9270	0.9597	-
e^{N_h, M_τ}	1.0773e-01	6.3940e-02	3.5427e-02	1.8633e-02	9.5803e-03
R^{N_h, M_τ}	0.7526	0.8519	0.9270	0.9597	-

A boundary layer, as shown in Figures 1 and 2, is located at the right side of the space domain in the numerical solution of Examples 1 and 2 above. Figures 1 and 2 also display the computed solutions $W_{i,j}$ for various perturbation parameter values, along with the influence of fractional order. Figure 3 displays the log-log plots of the maximum absolute errors against the number of meshes for both cases, demonstrating the developed numerical scheme's convergent nature regardless of the perturbation value. The suggested scheme is ε-uniformly convergent, as illustrated by the numerical results shown in Tables 1 and 2, by combining the midpoint upwind numerical method in the spatial direction with the implicit Euler's method in the temporal direction. We can see that, for each value of ε, the maximum pointwise error decreases as N and M grow, from the results in Tables 1 and 2.

Table 2: Maximum error and rate of convergence for various ε values with a fixed $\gamma = 0.5$ for Example 2.

$N_h = M_\tau \Rightarrow$	32	64	128	256	512
$\varepsilon = 1$	4.6381e-03	2.0344e-03	9.4019e-04	4.5021e-04	2.2007e-04
	1.1889	1.1136	1.0623	1.0327	-
$\varepsilon = 2^{-4}$	4.7943e-02	2.3827e-02	1.2645e-02	6.8350e-03	3.6952e-03
	1.0088	0.9140	0.8875	0.8873	-
$\varepsilon = 2^{-8}$	6.3770e-02	2.8254e-02	1.2921e-02	6.1518e-03	3.0787e-03
	1.1744	1.1288	1.0706	0.9987	-
$\varepsilon = 2^{-10}$	6.6336e-02	3.0540e-02	1.3973e-02	6.7869e-03	3.3299e-03
	1.1191	1.1280	1.0418	1.0272	-
$\varepsilon = 2^{-12}$	6.7001e-02	3.1194e-02	1.4619e-02	6.9617e-03	3.4446e-03
	1.1029	1.0934	1.0703	1.0151	-
$\varepsilon = 2^{-14}$	6.7211e-02	3.1406e-02	1.4841e-02	7.1616e-03	3.5058e-03
	1.0976	1.0815	1.0512	1.0306	-
$\varepsilon = 2^{-20}$	6.7224e-02	3.1420e-02	1.4855e-02	7.1765e-03	3.5212e-03
	1.0973	1.0808	1.0496	1.0272	
$\varepsilon = 2^{-24}$	6.7225e-02	3.1421e-02	1.4856e-02	7.1775e-03	3.5222e-03
	1.0973	1.0807	1.0495	1.0270	-
$\varepsilon = 2^{-26}$	6.7225e-02	3.1421e-02	1.4856e-02	7.1775e-03	3.5223e-03
	1.0973	1.0807	1.0495	1.0270	-
$\varepsilon = 2^{-30}$	6.7225e-02	3.1421e-02	1.4856e-02	7.1775e-03	3.5223e-03
	1.0973	1.0807	1.0495	1.0270	-
e^{N_h, M_τ}	6.7225e-02	3.1421e-02	1.4856e-02	7.1775e-03	3.5223e-03
R^{N_h, M_τ}	1.0973	1.0807	1.0495	1.0270	-

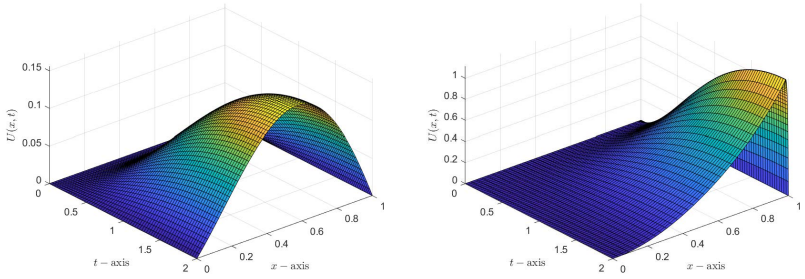

(a) $\varepsilon = 2^0$ (b) $\varepsilon = 2^{-6}$

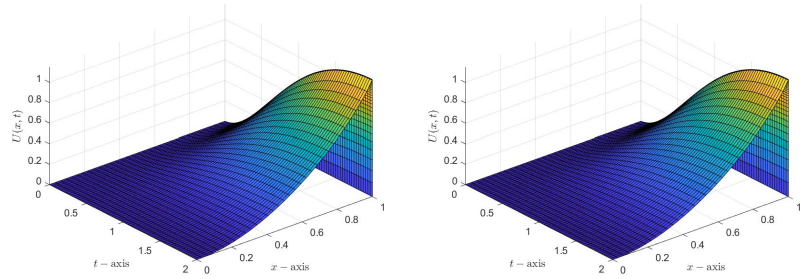

(c) $\varepsilon = 2^{-10}$ (d) $\varepsilon = 2^{-20}$

Figure 2: A three-dimensional representation of the numerical solution for Example 2 for various ε values with $\gamma = 0.5$, $M_x = 32$, and $M_t = 40$.

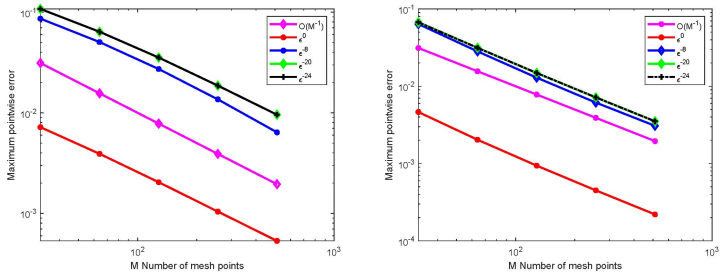

(a) Log-log plot of the max error for Example 1 (b) Log-log plot of the max error for Example 2

Figure 3: Log-log plot of maximum absolute errors for Examples 1 and 2 for different values of ε.

It is evident that, for every N, M, the maximum point-wise error is $\varepsilon \longrightarrow 0$ stable. By utilizing these two examples, we verify that the suggested numerical technique is more accurate, stable, and ε-uniformly convergent, with a convergence rate that is almost one. The maximum point-wise error is stable for all N, M. Using these two cases, we demonstrate that the proposed numerical technique is accurate, stable, and ε-uniformly convergent, with a convergence rate of almost one.

7 Conclusion

The time delay singularly perturbed parabolic convection-diffusion problem with time-fractional derivative order was solved using the midpoint upwind numerical approach. The solution to the problem depicted a boundary layer on the right side of the spatial domain. The solution's layer region has a steep gradient due to the presence of ε. Because of the frequently changing solution behavior in the layer region, it is computationally difficult to calculate the solution analytically or using traditional numerical methods. To mitigate this effect, we devised a strategy that employs the midway upwind scheme in the spatial direction and an implicit Euler's scheme in the temporal direction. The established numerical technique has been proven to be stable and uniformly convergent. To confirm the method's compatibility, two model problems were considered for numerical testing at varied perturbation parameters and fractional-order derivative values. Tables 1 and 2 provide a summary of the numerical results, including maximum absolute errors and numerical rate of convergence. Furthermore, the log-log plot (Figure 3) and the numerical solution for Examples 1 and 2 (refer to Figures 1 and 2) indicate the ε-uniform convergence of the scheme. The scheme's order of convergence is $O(N^{-1} + \tau)$, and it is uniformly convergent at ε. The devised scheme provides more stable, accurate, and uniformly convergent numerical results.

Acknowledgments

The authors would like to thank the anonymous reviewers for their helpful feedback and recommendations that helped to make the article more successful.

References

[1] Al-Mdallal, Q. and Syam, M. *An efficient method for solving non-linear singularly perturbed two points boundary-value problems of fractional order,* Commun. Nonlinear Sci. Numer. Simul. 17(6) (2012) 2299–2308.

[2] Atangana, A. and Goufo, E. *Extension of matched asymptotic method to fractional boundary layers problems,* Math. Probl. Eng. 2014 (1) (2014) 107535.

[3] Bijura, A.M. *Nonlinear singular perturbation problems of arbitrary real orders,* 2003.

[4] Caputo, M. and Fabrizio, M. *A new definition of fractional derivative without singular kernel,* Progr. Fract. Differ. Appl. 1(2) (2015) 73–85.

[5] Cooke, K. *Differential—difference equations,* In International symposium on nonlinear differential equations and nonlinear mechanics, pages 155–171. Elsevier, 1963.

[6] Diekmann, O., Gils, S., Lunel, S. and Walther, H. Delay equations: functional-, complex-, and nonlinear analysis, volume 110. Springer Science & Business Media, 2012.

[7] Driver, R. *Ordinary and delay differential equations*, volume 20. Springer Science & Business Media, 2012.

[8] Gelu, F. and Duressa, G. *Hybrid method for singularly perturbed robin type parabolic convection–diffusion problems on shishkin mesh,* Partial Differ. Equ. Appl. Math. 8 (2023) 100586.

[9] Govindarao, L. and Mohapatra, J. *A second order numerical method for singularly perturbed delay parabolic partial differential equation,* Eng. Comput. 36(2) (2019) 420–444.

[10] Hailu, W. and Duressa, G. Accelerated parameter-uniform numerical method for singularly perturbed parabolic convection-diffusion problems with a large negative shift and integral boundary condition. Result. Appl. Math. 18 (2023) 100364.

[11] Hailu, W. and Duressa, G. *Uniformly convergent numerical scheme for solving singularly perturbed parabolic convection-diffusion equations with integral boundary condition,* Differ. Equ. Dyn. Syst. (2023) 1–27 .

[12] Hailu, W. and Duressa, G. *A robust collocation method for singularly perturbed discontinuous coefficients parabolic differential difference equations,* Research in Mathematics, 11(1) (2024) 2301827.

[13] Hale, J. and Lunel, S. *Introduction to functional differential equations*, volume 99. Springer Science & Business Media, 2013.

[14] Hassen, Z. and Duressa, G. *Parameter uniform hybrid numerical method for time-dependent singularly perturbed parabolic differential equations with large delay,* Appl. Math. Sci. Eng. 32(1) (2024) 2328254.

[15] Kolmanovskii, V. and Myshkis, A. *Applied theory of functional differential equations*, volume 85. Springer Science & Business Media, 2012.

[16] Kolmanovskii, V. and Nosov, V. *Stability of functional differential equations*, volume 180. Elsevier, 1986.

[17] Kuang, Y. *Delay differential equations: with applications in population dynamics*. Academic press, 1993.

[18] Kumar, K. and Vigo-Aguiar, J. *Numerical solution of time-fractional singularly perturbed convection–diffusion problems with a delay in time,* Math. Method. Appl. Sci. 44(4) (2021) 3080–3097.

[19] Losada, J. and Nieto, J. *Properties of a new fractional derivative without singular kernel,* Progr. Fract. Differ. Appl. 1(2) (2015) 87–92.

[20] Meerschaert, M. and Tadjeran, C. *Finite difference approximations for two-sided space-fractional partial differential equations,* Applied numerical mathematics, 56(1) (2006) 80–90.

[21] Miller, J., O'riordan, E, and Shishkin, G. *Fitted numerical methods for singular perturbation problems: error estimates in the maximum norm for linear problems in one and two dimensions.* World scientific, 2012.

[22] Miller, P. *Applied asymptotic analysis*, volume 75. American Mathematical Soc., 2006.

[23] Negero, N. and Duressa, G. *A method of line with improved accuracy for singularly perturbed parabolic convection–diffusion problems with large temporal lag,* Results Appl. Math. 11 (2021) 100174.

[24] Negero, N. and Duressa, G. *An exponentially fitted spline method for singularly perturbed parabolic convection-diffusion problems with large time delay,* Tamkang J. Math., 54(4) (2023) 313–338.

[25] Nelson, P. and Perelson, A. *Mathematical analysis of delay differential equation models of HIV-1 infection,* Math.Biosci., 179(1) (2002) 73–94.

[26] Norkin, S. *Introduction to the theory and application of differential equations with deviating arguments.* Academic Press, 1973.

[27] Podlubny, I. *Fractional differential equations: an introduction to fractional derivatives, fractional differential equations, to methods of their solution and some of their applications.* elsevier, 1998.

[28] Podlubny, I. *An introduction to fractional derivatives, fractional differential equations, to methods of their solution and some of their applications,* Math. Sci. Eng. 198 (1999) 1-340.

[29] Rangaig, N. and Pido, A. *Finite difference approximation method for two-dimensional space-time fractional diffusion equation using nonsingular fractional derivative.* Prog. Fract. Differ. Appl, 5(4) (2019) 1–11.

[30] Roop, J. *Numerical approximation of a one-dimensional space fractional advection–dispersion equation with boundary layer,* Comput. Math. Appl. 56(7) (2008) 1808–1819.

[31] Roos, H., Stynes, M. and Tobiska, L. *Robust numerical methods for singularly perturbed differential equations: convection-diffusion-reaction and flow problems*, volume 24. Springer Science & Business Media, 2008.

[32] Sadri, K. and Aminikhah, H. *An efficient numerical method for solving a class of variable-order fractional mobile-immobile advection-dispersion equations and its convergence analysis,* Chaos, Solitons Fractals, 146 (2021) 110896.

[33] Sahoo, S. and Gupta, V. *A robust uniformly convergent finite difference scheme for the time-fractional singularly perturbed convection-diffusion problem,* Comput. Math. Appl. 137 (2023) 126–146.

[34] Sayevand, K. and Pichaghchi, K. *Efficient algorithms for analyzing the singularly perturbed boundary value problems of fractional order,* Commun. Nonlinear Sci. Numer. Simul., 57 (2018) 136–168.

[35] Sayevand, K. and Pichaghchi, K. *A novel operational matrix method for solving singularly perturbed boundary value problems of fractional multi-order,* Int. J. Comput. Math. 95(4) (2018) 767–796.

[36] Shakti, D., Mohapatra, J., Das, P. and Vigo-Aguiar, J. *A moving mesh refinement based optimal accurate uniformly convergent computational method for a parabolic system of boundary layer originated reaction–diffusion problems with arbitrary small diffusion terms,* J. Comput. Appl. Math. 404 (2022) 113167.

[37] Villasana, M. and Radunskaya, A. *A delay differential equation model for tumor growth,* J. Math. Bio. 47 (2003) 270–294.

[38] Yuste, S. and Acedo, L. *An explicit finite difference method and a new von neumann-type stability analysis for fractional diffusion equations,* SIAM J. Numer. Anal. 42(5) (2005) 1862–1874.

[39] Zhao, T. *Global periodic-solutions for a differential delay system modeling a microbial population in the chemostat,* J. Math. Anal. Appl. 193(1) (1995) 329–352.